Article

Microwave Synthesis of CdSe and CdTe Nanocrystals in Nonabsorbing Alkanes

Aaron L. Washington II, and Geoffrey F. Strouse

J. Am. Chem. Soc., **2008**, 130 (28), 8916-8922 • DOI: 10.1021/ja711115r • Publication Date (Web): 25 June 2008

J|A|C|S
ARTICLES

Published on Web 06/25/2008

Microwave Synthesis of CdSe and CdTe Nanocrystals in Nonabsorbing Alkanes

Aaron L. Washington II and Geoffrey F. Strouse*

Department of Chemistry and Biochemistry, Florida State University, Tallahassee, Florida 32306-4390

Received December 26, 2007; E-mail: Strouse@chem.fsu.edu

Abstract: Controlling nanomaterial growth via the "specific microwave effect" can be achieved by selective heating of the chalcogenide precursor. The high polarizability of the precursor allows instantaneous activation and subsequent nucleation leading to the synthesis of CdSe and CdTe in nonmicrowave absorbing alkane solvents. Regardless of the desired size, narrow dispersity nanocrystals can be isolated in less than 3 min with high quantum efficiencies and elliptical morphologies. The reaction does not require a high temperature injection step, and the alkane solvent can be easily removed. In addition, batch-to-batch variance in size is 4.2 ± 0.14 nm for 10 repeat experimental runs. The use of a stopped-flow reactor allows near continuous automation of the process leading to potential industrial benefits.

1. Introduction

Over the past decade, there has been a vast amount of work to optimize the synthetic methodology for the II−VI (CdS,[1] CdSe,[2] CdTe[3]) nanocrystalline semiconductors, leading to commercially available materials and applications for a wide range of technologies.[4–6] The synthetic methods for preparation of nanocrystals have improved by optimizing the reagents, ligands, solvents, and the general approach.[2b,7–9] The initial synthetic breakthrough in the control of size dispersity by Murray[10] led to the recent results demonstrating the use of nonorganometallic precursors for preparation of CdSe based on CdO or Cd stearate by the research group of Peng.[11] Breakthroughs by Alivisatos,[12] Hyeon,[13] El-Sayed,[14] and Peng[15] have shown remarkable control over the shape and morphology of the nanocrystals. Cao et al.[16] and Hyeon[13] have demonstrated the ability to produce nanomaterials without the hot injection step allowing the nanocrystals to be efficiently prepared. These routes all have demonstrated the ability to produce nanocrystals of high quality as measured by emissive quantum efficiency and size dispersity with reactions that can be reproduced universally at a macroscopic level for a given material (narrow size dispersity with defined crystallinity); however, at the microscopic level the materials are not identical batch-to-batch (identical size, identical shape) and may vary as a function of heating rate, mixing rate, and concentrations. In other words, the size and aspect ratio (shape) vary with each reaction reminiscent of a polymer chemistry problem; however, one can isolate nearly the same size if the absorption is actively monitored.[17]

(1) (a) Lazell, M.; O'Brien, P. *J. Mater. Chem.* **1999**, *9*, 1381–1382. (b) Cumberland, S. L.; Hanif, K. M.; Javier, A.; Khitrov, G. A.; Strouse, G. F.; Woessner, S. M.; Yun, C. S. *Chem. Mater.* **2002**, *14*, 1576–1584. (c) Yu, W. W.; Peng, X. *Angew. Chem., Int. Ed.* **2002**, *41* (13), 2368–2371.

(2) (a) Peng, Z. A.; Peng, X. *J. Am. Chem. Soc.* **2002**, *124*, 2049–2055. (b) Qu, L.; Peng, X. *J. Am. Chem. Soc.* **2002**, *124*, 2094–2095. (c) Dabbousi, B. O.; Rodriguez-Viego, J.; Mikulee, F. V.; Heine, J. R.; Mattoussi, H.; Ober, R.; Jensen, K. F.; Bawendi, M. G. J. *Phys. Chem. B* **1997**, *101*, 9463–9475.

(3) (a) Gao, M; Kirstein, S; Mohwald, H; Rogach, A. L.; Kornowski, A; Eych|Aamller, A; Weller, H. *J. Phys. Chem. B* **1998**, *102*, 8360–8363. (b) He, Y; Sai, L.; Lu, H.; Hu, M.; Lai, W.; Fan, Q.; Wang, L.; Huang, W. *J. Phys Chem. B* **2006**, *110* (27), 13352–13356. (c) He, Y; Sai, L.; Lu, H.; Hu, M.; Lai, W.; Fan, Q.; Wang, L.; Huang, W. *J. Phys. Chem. B* **2006**, *110* (27), 13370–13374. (d) Li, L.; Qian, H.; Ren, J. *Chem. Commun. (Cambridge, UK)* **2005**, (4), 528–530.

(4) (a) Diguna, L J.; Shen, Q.; Kobayashi, J.; Toyoda, T. *Appl. Phys. Lett.* **2007**, *91* (2), 023116/1−023116/3. (b) Leschkies, K. S.; Divakar, R.; Basu, J.; Enache-Pommer, E.; Boercker, J. E.; Carter, C. B.; Kortshagen, U. R.; Norris, D. J.; Aydil, E. S. *Nano Lett.* **2007**, *7* (6), 1793–1798.

(5) (a) Kronik, L.; Ashkenasy, N.; Leibovitch, M.; Fefer, E; Shapira; Yoram; Gorer, S.; Hodes, G. *J. Electrochem. Soc.* **1998**, *145* (5), 1748–1755. (b) Gao, Xiaohu; Chan, W. C. W.; Shuming, N. *J. Biomed. Opt.* **2002**, *7* (4), 532–537.

(6) (a) Liang, Hongjun; Angelini, Thomas E; Ho, James; Braun, Paul V; Wong, Gerard C. L. *J. Am. Chem. Soc.* **2003**, *125* (39), 11786–11787. (b) Sandros, M. G.; Gao, D.; Benson, D. E. *J. Am. Chem. Soc.* **2005**, *127* (35), 12198–12199.

(7) (a) Yu, W. W.; Wang, Y. A.; Peng, X. *Chem. Mater.* **2003**, *15* (22), 4300–4308. (b) Pradhan, N.; Reifsnyder, D.; Xie, R.; Aldana, J.; Peng, X. *J. Am. Chem. Soc.* **2007**, *129* (30), 9500–9509.

(8) (a) Munro, A. M.; Plante, I. J.; Ng, M. S.; Ginger, D. S. *J. Phys. Chem. C* **2007**, *111* (17), 6220–6227. (b) Kalyuzhny, G.; Murray, R. W. *J. Phys. Chem. B* **2005**, *109* (15), 7012–7021.

(9) (a) Gao, X.; Chan, W. C. W.; Shuming, N. *J. Biomed. Opt.* **2002**, *7* (4), 532–537. (b) Liang, H.; Angelini, T. E.; Ho, J.; Braun, P. V.; Wong, G. C. L. *J. Am. Chem. Soc.* **2003**, *125* (39), 11786–11787. (c) Sandros, M. G.; Gao, D.; Benson, D. E. *J. Am. Chem. Soc.* **2005**, *127* (35), 12198–12199.

(10) Murray, C. B.; Norris, D. J.; Bawendi, M. G. *J. Am. Chem. Soc.* **1993**, *115* (19), 8706–8715.

(11) Peng, Z. A.; Peng, X. *J. Am. Chem. Soc.* **2001**, *123* (1), 183–184.

(12) Peng, X.; Manna, U.; Yang, W.; Wickham, J.; Scher, E.; Kadavanich, A.; Allvisatos, A. P. *Nature (London)* **2000**, *404* (6773), 59–61.

(13) (a) Park, J.; An, K.; Hwang, Y.; Park, J.-G.; Noh, H.-J.; Kim, J.-Y.; Park, J.-H.; Hwang, N.-M.; Hyeon, T. *Nat. Mater.* **2004**, *3* (12), 891–895. (b) Park, J.; Joo, J.; Kwon, S. G.; Jang, Y.; Hyeon, T. *Angew. Chem, Int. Ed.* **2007**, *46* (25), 4630–4660.

(14) Mohamed, M. B.; Burda, C.; El-Sayed, M. A. *Nano Lett.* **2001**, *1* (11), 589–593.

(15) Peng, Z. A.; Peng, X. *J. Am. Chem. Soc.* **2001**, *123* (7), 1389–1395.

(16) (a) Yang, Y. A.; Wu, H.; Williams, K. R.; Cao, Y. C. *Angew. Chem., Int. Ed.* **2005**, *44* (41), 6712–5. (b) Cao, Y. C.; Wang, J. *J. Am. Chem. Soc.* **2004**, *126* (44), 14336–14337.

10.1021/ja711115r CCC: $40.75

The reaction mechanism for nanocrystal growth implies that the growth behavior should be microscopically controllable if the reaction mechanism including contributions from precursor activation, nucleation, and growth are controlled.[18] However, variance in heating rate, cooling rate, thermal gradients in the reaction, and differences in injection rate lead to size and shape variation from batch-to-batch. We have demonstrated that the use of dielectric (microwave) versus convective heating is advantageous to controlling many of the above heating variances that impact material dispersity.[19,20] In our earlier study, we developed microwave chemistry for nanocrystals showing rate acceleration for InP, InGaP, and CdSe by addition of ionic liquids or use of ionic precursors. However, organic chemists have shown not only rate improvements but also, more importantly, an exquisite synthetic control over the product formation can be achieved by selectively heating a polar transition state or precursor in the microwave (MW) to allow a selected product to be isolated. The selectivity offered by MW heating demonstrates the "specific microwave effect."[21] This is defined as the ability to selectively heat molecular precursors that are highly polarizable in the presence of molecules that are less polarizable. The specific microwave effect is advantageous in controlling the batch-to-batch variation in nanocrystal production, particularly if selective heating allows the nucleation event to be specifically triggered by the MW and thereafter allowing growth to proceed.

The use of MW irradiation has several unique advantages over convective heating: (1) selective activation of the target precursor to initiate nucleation and subsequent growth, (2) reproducibility from batch-to-batch, (3) the convenience of a noninjection reaction, and (4) a stopped-flow near-continuous nanocrystal synthesis. The demonstration of the selective triggering of nanocrystal nucleation and growth by choosing a molecular chalcogenide source to be the only reactant with significant MW absorption allows the manifestation of the "specific microwave effect" for nanocrystal preparation. The chalcogenide precursor selectively absorbs the microwave energy, which appears to result in the instantaneous nucleation and growth upon microwave irradiation. The nanocrystals can be grown rapidly and controlled by a combination of reactant concentration and power, while size is dictated by the reaction temperature. Selective absorption by the chalcogenide results in the isolation of elliptical (aspect ratio 1.2) CdSe and elliptical (aspect ratio 1.7) CdTe in the size range 2.5−8 nm. The materials are prepared in less than 3 min with a typical out-of-reactor dispersity of 6% for CdSe (12% for CdTe) but, more importantly,with a standard deviation in size for the CdSe (CdTe) reaction of 4.2 ± 0.14 nm (4.25 ± 0.3 nm) from batch-to-batch (averaged over 10 individual runs). It is important to note that the size dispersity reflects the batch composition without attempting to size select the materials via selective precipitation. Although Cao[16] has demonstrated noninjection routes for convectively grown CdSe and CdTe nanocrystals, the MW reaction can utilize a similar approach, but via the use of a pump, the reactants can be continuously delivered. This allows application of the MW to a stopped-flow synthetic technique allowing continuous preparation of the material at a rate of 650 mg/h. The reproducibility from batch-to-batch of the method and the ability to continuously synthesize nanocrystals are fascinating, particularly for the potential automation of synthesis of these materials.

2. Experimental Section

2.1. Chemicals. All reactants and solvents were used without further purification. Cadmium stearate (CdSA, 90%), selenium powder (Se, 99.99%), and cadmium nitrate tetrahydrate ($CdNO_3$, 98%) were both purchased from Strem Chemicals. Tri-*n*-octylphosphine (TOP, 90%), tri-*n*-butylphosphine (TBP, 93%), cadmium oxide (CdO, 99.998%), and selenourea (SeU, 99.9%) were purchased from Alfa Aesar. Decane (99%), *n*-octane (99%), hexadecylamine (HDA, 90%), and tellurium powder (Te, 99%) were all purchased from Acros Organics. Heptane (HPLC grade) was purchased from EMD Chemicals. Pentane (HPLC grade) was purchased from Fisher Scientific. Octylamine was purchased from Sigma Aldrich.

2.2. Characterization. Isolation of all nanocrystals is achieved by addition of minimal amounts of toluene followed by the addition of a methanol and butanol mixture to induce particle precipitation. The precipitate was collected via centrifugation and decantation of the supernatant. This process was repeated two more times with toluene/methanol to ensure reagent-free particles. Absorption measurements were performed on a Varian Cary 50 UV−vis spectrophotometer. Photoluminescence measurements were performed on a Varian Cary Eclipse Fluorescence spectrophotometer using quartz cuvettes (cell path length = 1 cm). X-ray diffraction were recorded on 10 mg samples on a Rigaku DMAX 300 Ultima III Powder X-ray diffractometer (using Cu Kα $\lambda = 1.5418$ Å radiation). The transmission electron micrographs (TEM) were obtained using a Philips CM 300-field emission gun with a maximum acceleration voltage of 300 keV. A Gatan 673 wide angle CCD camera (Tietz Tem-Cam F415/MP slow scan) with a field of view of 61 mm × 61 mm was used to digitize the micrographs. TEM samples were prepared as dilute solutions in toluene with an absorbance of less than 0.1 to prevent aggravation. One drop of the prepared solution was placed onto a holey carbon 400 mesh TEM grid for 1 min, and the drop was removed. The TEM sample was dried overnight in a desiccator prior to imaging.

2.3. Microwave. All microwave syntheses was performed in a single mode CEM Discover System operating at 300 W, 2.45 GHz. The microwave operates up to 300 °C and 300 psi. The reaction was carried out either in a static 10 mL reaction vessel (4−5 mL reaction volume) or dynamically in the 80 mL vessel (50 mL reaction volume) coupled to a stopped-flow pump (CEM Voyager) in which individual precursors can be delivered in to the reaction chamber using a peristaltic pump. The reaction is rapidly cooled using high pressure air (40 psi) following termination of the reaction. The solvent temperature is actively monitored. While the conditions are instrument dependent, the reproducibility for the CEM microwave is remarkable allowing instantaneous application of the method with minimal method development. The synthesized material must be optimized to individual microwave systems in terms of reaction time and power, to obtain the highest quality and best dispersity.

2.4. Static Reactions. 2.4.1. Synthesis of CdSe. Nanocrystalline CdSe was prepared by adaptation of the reported method of Peng et al., with the substitution of alkane solvents (pentane, heptane, octane, decane), cadmium stearate (CdSA), and microwave based dielectric heating.[2a] Briefly, stock solutions of CdSA and TOPSe

(17) Qu, L.; Yu, W. W.; Peng, X. *Nano Lett.* **2004**, *4* (3), 465–469.
(18) Peng, Z. A.; Peng, X. *J. Am. Chem. Soc.* **2002**, *124* (13), 3343–3353.
(19) (a) Gerbec, J. A.; Magana, D.; Washington, A.; Strouse, G. F. *J. Am. Chem. Soc.* **2005**, *127* (45), 15791–15800. (b) Ziegler, J.; Merkulov, A.; Grabolle, M.; Resch-Genger, U.; Nann, T. *Langmuir* **2007**, *23* (14), 7751–7759. (c) Zhu, J.; Palchik, O.; Chen, S.; Gedanken, A. *J. Phys. Chem. B* **2000**, *104* (31), 7344–7347.
(20) (a) Jiang, Y.; Zhu, Y. *Chem. Lett.* **2004**, *33* (10), 1390–1391. (b) Chu, M.; Shen, X.; Liu, G. *Nanotechnology* **2006**, *17* (2), 444–449. (c) Wang, Q.; Seo, D. *Chem. Mater.* **2006**, *18* (24), 5764–5767. (d) Rogach, A. L.; Nagesha, D.; Ostrander, J. W.; Giersig, M.; Kotov, N. A. *Chem. Mater.* **2000**, *12*, 2676–2685.
(21) (a) De La Hoz, A.; Diaz-Ortiz, A.; Moreno, A. *Curr. Org. Chem.* **2004**, *8* (10), 903–918. (b) Desai, B.; Danks, T. N.; Wagner, G. *Dalton Trans.* **2004**, (1), 166–171. (c) Yadav, G. D.; Bisht, P. M. *J. Mol. Catal. A: Chem.* **2005**, *236* (1−2), 54–64.

were prepared by dispersing CdSA (1.0 mmol, 679.36 mg) into 20 mL of an alkane of choice by sonication, while a 1 M solution of TOPSe was prepared under argon using Se powder (0.01mol) dissolved in 10 mL of TOP. The reaction mixture was added to a 10 mL reaction vessel under ambient conditions consisting of a 1:5 molar ratio of cadmium to selenium stock solutions with HDA (hexadecylamine) added in an equimolar ratio to TOP. The reaction mixture was heated in the microwave cavity to a temperature of 240 °C during a 30 s ramp period at a power of 300 W. The mixture was then allowed to react for 30 s at 240 °C and immediately cooled to room temperature (<1 min) using forced air cooling. Isolation of the nanocrystals was carried out by standard reprecipitation methods. The reaction yields elliptical (aspect ratio of 1.2) CdSe nanocrystals with a 6% size dispersity and 35 ± 5 mg of sample per 4 mL reaction volume.

2.4.2. Synthesis of CdTe. CdTe is prepared analogously to the reaction above, with the exception that a 25 mM CdSA in decane stock solution is prepared. The Te stock solution (1 M TOP/Te) is prepared under Ar by heating tellurium powder (0.005mol) in 10 mL of TOP at 100 °C for 24 h. The stock solutions were mixed in a 1:1 molar ratio with HDA (equimolar to the TOP). This reaction mixture is heated in the microwave to 220 °C, at 300 W, and allowed to react for 5 s. The reaction was immediately cooled to room temperature. Isolation of the nanocrystals was carried out by standard reprecipitation methods. The CdTe reaction yields 25 ± 5 mg of elliptical (aspect ratio of 1.7) nanocrystals with a 12% size dispersity per 4 mL reaction volume.

2.5. Stopped-Flow Synthesis. The static MW synthetic method can be adapted to a stop-flow pump system by substitution of octylamine for HDA in the cadmium stock solution, in order to dissolve the CdSA dispersion. The TOPSe stock and CdSA stock are delivered into the reaction chamber form separate sources to fill a 50 mL reaction volume and heated to 190 °C at 300 W for 40 min. Longer reaction times are needed due to the pathway of the solvent scattering the microwave energy and a thicker reaction vessel. The reaction mixture is pumped out to a sealed vessel under argon. Collection of the nanocrystals is achieved by precipitation using standard methods. Continuous transfer of stock and product can be carried out in the stopped-flow allowing continuous production of a target nanocrystal. The yield of nanocrystals is ~650 mg/h.

3. Results and Discussion

In the field of microwave (MW) chemistry, much effort has focused on the tailoring of the reactants polarizability differences to produce a desired product via the specific microwave effect. The highest polarizable material will selectively absorb MW energy in the presence of poorly absorbing materials and solvents. The absorption of MW energy by a polarizable reactant provides the requisite energy to overcome potential activation barriers associated with the transition state or reactive intermediates. Although the specific microwave effect is prolific in the literature,[22] proving the effect is very challenging. In order to take advantage of the specific microwave effect for nanocrystal synthesis, particularly for high throughput synthesis, the reactive precursors must be strong microwave absorbers, while the solvent must be nonabsorptive (Figure 1). The excess energy controlled by the solvent allows for continuous growth resulting in a reverse thermal gradient and eliminates multiple nucleation events that can lead to loss of material dispersity.

The advantage of the "*specific microwave effect*" for nanocrystals can be understood by considering the mechanism for

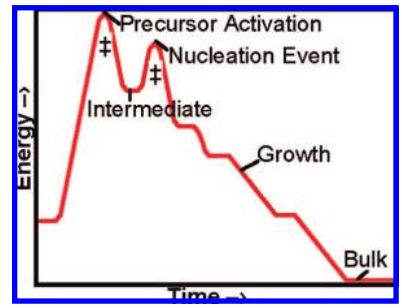

Figure 1. Schematic diagram illustrating the reaction pathway for nanocrystal formation.

the formation of the nanocrystal.[23b] In the simplest projection of a rather complex reaction mechanism, the primary steps in a nanocrystal reaction are precursor activation, nanocrystal nucleation, and passivant controlled atom addition onto the growing nanocrystal facets (Figure 1). In the case of nanocrystal growth, the selective heating translates into a controlled nucleation event, thus eliminating the need for a high temperature injection step. Typically the limiting step for nanocrystal growth is the first two events (activation and nucleation),[20] depending on which step requires more energy. A critical reaction size must be reached to overcome the transition state barrier for activation and/or nucleation to occur before proceeding to product. While the rate of addition of the atoms to the surface is dependent on diffusion and thermodynamics, the rate of nanocrystal growth is controlled by reaction temperature and concentration, as well as the solubility product of the reactants and the surface energy of the binary semiconductor. Pressure can also play a role by enhancing products (small $\Delta V^{\ddagger}$) or inhibiting (larger $\Delta V^{\ddagger}$) reaction rates depending on the volume at the transition state, $\Delta V^{\ddagger}$. Nucleation theory predicts that a *critical* crystallite size must be achieved prior to sustained nanocrystal growth. Gamelin et al. has demonstrated the applicability of nucleation theory to describing nanocrystal growth.[24] The nucleation event is a kinetic problem, where the rate of growth must exceed the rate of dissolution for nanocrystal nucleation to occur.[21] The nucleation transition state is influenced by the chemical activity of the precursor, as shown by Peng[21,25] and Cao,[16] and can therefore be used to control the nucleation event by introducing a barrier to nucleation. For a lyothermal reaction, the energy required for nucleation is provided indirectly through convective heating of the precursors via solvent heating. To achieve controlled growth after nucleation, lyothermal methods rely on induced cooling upon injection of the precursors. For a convective reaction, the subsequent steps are dictated by precursor activity.

A higher level of control can be achieved in a microwave reaction if the energy barrier is larger for the precursor activation than the nucleation event. In this regime, the specific microwave effect can be utilized to drive a reaction by selectively activating a desired precursor to initiate nucleation. Since the precursor is only activated under microwave irradiation (the cleavage of the TOP−Se or TOP−Te bond),[26] the accessibility of the chalco-

(22) (a) de la Hoz, A.; Diaz-Ortiz, A.; Moreno, A. *Chem. Soc. Rev.* **2005**, *34* (2), 164–178. (b) Pchelka, B. K.; Loupy, A.; Petit, A. *Tetrahedron* **2006**, *62* (47), 10968–10979.

(23) (a) Talapin, D. V.; Shevchenko, E. V.; Murray, C. B.; Kornowski, A.; Foerster, S.; Weller, H. *J. Am. Chem. Soc.* **2004**, *126* (40), 12984–12988. (b) Peng, X.; Wickham, J.; Alivisatos, A.P. *J. Am. Chem. Soc.* **1998**, *120* (21), 5343–5344.

(24) Bryan, J. D.; Gamelin, D. R. *Prog. Inorg. Chem.* **2005**, *54*, 47–126.

(25) (a) Chen, Y.; Johnson, E.; Peng, X. *J. Am. Chem. Soc.* **2007**, *129* (35), 10937–10947. (b) Joshi, S.; Sen, S.; Ocampo, P. C. *J. Phys. Chem. C* **2007**, *111* (11), 4105–4110.

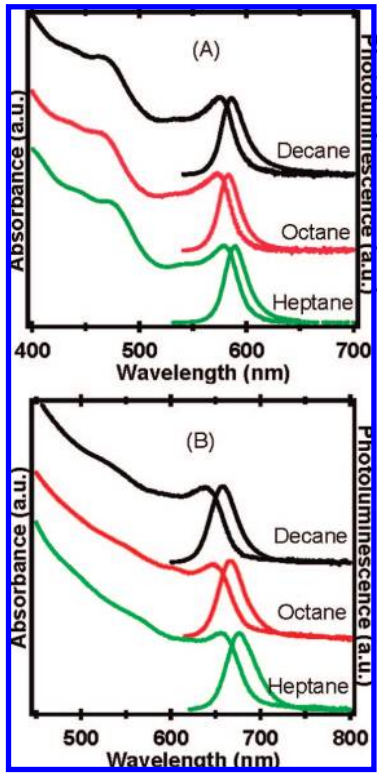

Figure 2. Optical absorption and photoluminescence of (A) CdSe and (B) CdTe using solvents of different alkyl chain lengths. CdSe/CdTe was grown at 240 °C/220 °C for 30 s/5 s with the power set to 300 W.

genide monomer to the growing nanocrystal is controlled by the MW cross section. This results in a remarkable degree of control over the reaction path. This requires that the precursor is the dominant absorber in the reaction and the solvent acts merely as a reaction moderator to control the explosive growth. It is also important in controlling growth that the evolving nanocrystal is also a moderate MW absorber, to ensure the reaction is under thermodynamic control. In effect, the absorption of the MW energy is the on−off switch for the reaction.

3.1. Preparation of CdSe (CdTe) Nanocrystals. In Figure 2, we demonstrate the ability to synthesize CdSe and CdTe nanocrystals in nonpolar, low boiling alkane solvents (decane, octane, heptane) in the microwave. CdSe and CdTe nanocrystals may also be prepared in pentane, but lower reaction temperatures are required due to reactor pressurization limits, thus generating a smaller range of achievable nanocrystal sizes under the current microwave design (Supporting Figure 1). There is no observed dependence on the optical properties or growth behavior as a function of the alkane solvent (with the exception of pentane), although pressurization of the reaction in the microwave occurs when the boiling point of the solvent is exceeded, which occurs in nearly every reaction.

The isolated nanocrystals are elliptical (aspect ratio 1.2) and exhibit narrow size dispersities (6% rms in CdSe, 12% rms in CdTe) based on TEM analysis (Supporting Figure 2). The CdSe crystal motif is wurtzite, while the CdTe is zinc blende (Supporting Figure 3). Nanocrystal size and structure are verified by powder X-ray diffraction using the Scherer expression and verified through TEM. The materials exhibit well-defined optical properties (line width, quantum yield) comparable to lyothermally grown materials and exhibit identical quantum efficiencies to materials grown by the traditional CdO lyothermal methods developed by Peng. The absorption data in Figures 2 and 3 are for the isolated batch rather than a size-selectively precipitated reaction, and the loss of the 1s−1p transition in comparison to the CdO grown materials (Supporting Figure 4) we believe reflects a combination of the slightly larger polydispersity of the material as well as the elliptical shape of the materials. The 1s−1p transition intensity, while a marker for monodispersity, is highly variable in the literature and as shown by Alivisatos,[21b] Cao,[16] and Ferreria[27] can be impacted by shape. A better measure of near monodispersity is the absorption line width for the 1s−1s exciton. For the MW grown CdSe the line width is 27−28 nm for the batch, which compares well with the absorption fwhm for Peng's CdO grown materials with an absorption line width of 27−28 nm (Supporting Figure 4). For CdTe the absorption line width is broader (40 nm) consistent with the larger polydispersity of the sample.

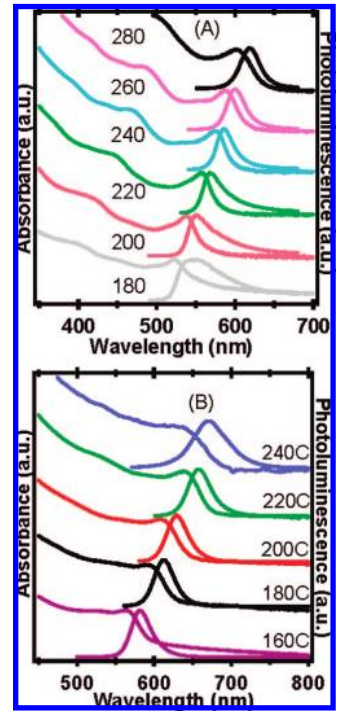

Figure 3. Optical data for temperature (°C) dependent growth of (A) CdSe and (B) CdTe. The reaction conditions include fixed power at 300 W and time at 30 s in the CdSe reactions and 5 s for CdTe.

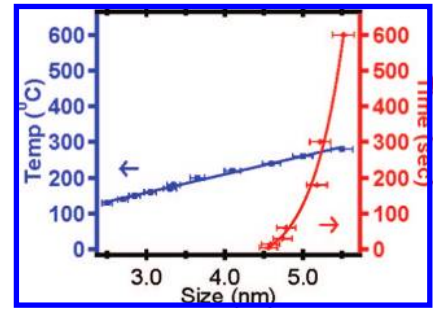

Figure 4. Size of CdSe is plotted against two parameters that are controlled during the microwave reaction: time (red) at a fixed temperature of 240 °C and temperature (blue) at a fixed time of 30 s.

(26) Liu, H.; Owen, J. S.; Alivisatos, A. P. *J. Am. Chem. Soc.* **2007**, *129* (2), 305–312.

(27) Ferreira, W. S.; de Sousa, J. S.; Freire, J. A. K.; Farias, G. A.; Freire, V. N. *Braz. J. Phys.* **2006**, *36* (2A), 438–439.

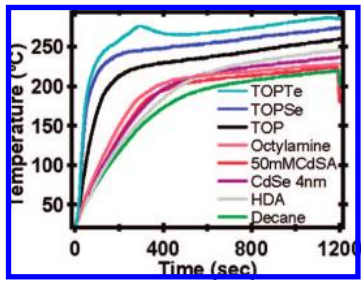

Figure 5. Microwave heating rates for different precursors, solvents, ligands, and nanocrystals in decane heated at 300 W.

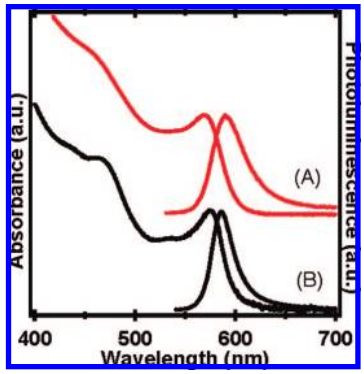

Figure 6. Absorption and photoluminescence spectra for (A) stop-flowed 80 mL and (B) conventional 10 mL reaction vessel.

In the microwave, the nanocrystal size is potentially influenced by reaction time, temperature, and applied power. The reaction temperature is the most critical of these parameters as shown in Figure 3, where the PL profile is broadened at low T. The MW power (200−300 W, Supporting Figure 5) and reaction time (CdSe: 5 s−10 min, CdTe 5 s−1 min, Supporting Figure 6) do not influence material size, shape, or quality. The quality of the materials is impacted if the ramp rate is altered; as nanocrystal growth occurs instantaneously in the reaction due to precursor activation and subsequent nucleation, reaction temperature requires thermal transfer to the solvent and exhibits a lag in response.

Other factors that influence the final material include the rate of cooling, the absence of microwave power, and the presence of nonabsorptive precursors.[18,28,29] Slow cooling from the reaction temperature to ambient conditions results in larger size dispersities. Such behavior is consistent with the domination of Ostwald ripening rather than MW precursor activation in the reaction once the MW power is removed. In the microwave, the presence of nonabsorptive precursors or low microwave power also leads to large polydispersities and poor optical performance, presumably due to the slow heating and multiple nucleation events in the reaction.

3.2. Implication for Mechanism. The enhanced reaction rates under MW irradiation either may reflect the control of the activation/nucleation step via selective heating with the excess energy leading to solvent heating or can effectively be a rapid solvent heating process leading to nucleation followed by an Ostwald ripening process. In Figure 4, a plot of the dependence on nanocrystal size is shown for two fixed points in the reaction parameter space, namely $P = 300$ W, reaction time = 30 s (blue) and $P = 300$ W, $T = 240$ °C (red).

Inspection of Figure 4 indicates that following nucleation the growth rate is linear with temperature, which is expected for a reaction under thermodynamic control where nanocrystal growth is determined by the diffusion of ions to the reactive nanocrystal surface. In the growth rate versus time plot a nonlinear, exponential dependence is observed implying the reaction is first-order. While this is unexpected for a convective reaction, where both cadmium and selenium should contribute to the overall order at nucleation (overall rate order = 2), it is not surprising for a microwave reaction if the rate limiting step is the precursor activation, namely the cleavage of the TOP−Se bond. This reduces the rate as the concentration of R_3P is reduced, leading to less MW energy being absorbed and thus fewer precursors to monomer production. If nucleation is dictated by the concentration and the selective absorption cross section for the precursor, then the microwave irradiation is enhancing the initial two steps.

Distinguishing between these two possibilities (activation versus nucleation) can be accomplished by analyzing the pressure dependent growth behavior in these reactions. Using the alkane as a pressure generator, due to boiling points, we observe that at high pressures the rate of reaction is slowed implying that one of the transition states has a large $\Delta V^{\ddagger}$.[30] This is logical for the nucleation step rather than the activation step, since a larger number of atoms must assemble for nanocrystal growth to begin. This suggests pressure may be used to manipulate the nucleation event. The result supports the assumption that nucleation is the critical reaction step for nanocrystal formation.[31]

3.3. Specific Microwave Effect. The absorbed microwave power (J/s) by a reagent can be related to the produced heat in time (Q) $dt = (mC\Delta T)\, dt$, where C is the specific heat, m is the mass, and T is temperature. The rate of heating ((Q) dt) is proportional to the MW absorption cross section using a simple Beer−Lambert law analogy, where $A = \epsilon bc$. The MW cross section in this equation is ϵ, and bc represent the precursor cross section or concentration per unit volume. The ramp rate to temperature depends on the absorptive cross section of the molecules in solution and the convective losses from the molecules to the solvent via thermal conduction. Thermal transfer depends on the thermal conductivity of the precursors.

The selectivity of microwave absorption by molecules in the reaction mixture can be observed in Figure 5 (Supporting Table 1) The rates of heating for TOP−Se and TOP−Te in decane are an order of magnitude larger than observed for just decane, HDA in decane, CdSA in decane, or the nanocrystals in decane indicative of selective microwave absorption for the most polarizable precursor. No experimental difference is observed for various nanocrystal sizes or concentration, suggesting the

(28) (a) Al-Salim, N.; Young, A. G.; Tilley, R. D.; McQuillan, A. J.; Xia, J. *Chem. Mater.* **2007**, *19* (21), 5185–5193. (b) Nag, A.; Sapra, S.; Chakraborty, S.; Basu, S.; Sarma, D. D. *J. Nanosci. Nanotechnol.* **2007**, *7* (6), 1965–1968. (c) Dai, Q.; Li, D.; Chen, H.; Kan, S.; Li, H.; Gao, S.; Hou, Y.; Liu, B.; Zou, G. *J. Phys. Chem. B* **2006**, *110* (33), 16508–16513. (d) Foos, E. E.; Wilkinson, J.; Maekinen, A. J.; Watkins, N. J.; Kafafi, Z. H.; Long, J. P. *Chem. Mater.* **2006**, *18* (12), 2886–2894.
(29) Deng, Z.; Cao, L.; Tang, F.; Zou, B. *J. Phys. Chem. B* **2005**, *109* (35), 16671–16675.
(30) (a) Granasy, L.; James, P. F. *J. Chem. Phys.* **2000**, *11321*, 9810–9821. (b) Yong-Sung, K.; Randolph, T. W.; Stevens, F. J.; Carpenter, J. F. *J. Biol. Chem.* **2002**, *277* (30), 27240–27246.
(31) (a) Shevchenko, E. V.; Talapin, D. V.; Schnablegger, H.; Kornowski, A.; Festin, O.; Svedlindh, P.; Haase, M.; Weller, H. *J. Am. Chem. Soc.* **2003**, *125* (30), 9090–101. (b) Yu, K.; Singh, S.i; Patrito, N.; Chu, V. *Langmuir* **2004**, *20* (25), 11161–11168. (c) He, Y.; Sai, L.; Lu, H.; Hu, M.; Lai, W.; Fan, Q.; Wang, L.; Huang, W. *Chem. Mater.* **2007**, *19* (3), 359–365.

microwave cross section for the nanocrystal is small. The low heating rate for decane, CdSA, and the alkyl amines is logical due to the low polarizability of these molecules leading to minute microwave absorption as evidenced in Figure 5 (or Supporting Table 1). CdSA shows little influence on heating rate over the alkane solvent and likewise has little impact on reaction temperature or precursor activation. The concentration dependence of CdSA shows a doubling of heating rate for a 5-fold increase in concentration, suggesting CdSA does absorb the MW energy, but is not a significant absorber in comparison to the phosphine chalcogenide. The rapid rate of heating for the tri-*n*-alkyl phosphine chalcogenide is predictable since it repeats the most polarizable molecule in the reaction mixture due to the large electronegativity differences between P and the chalcogenide. In fact, based on electronegativity arguments, one can predict that R_3P-Te is slower to heat than R_3P-Se, where the difference in rate is observed between TOP−Se and TOP−Te. This suggests that the heating of the reaction occurs only by thermal convection from the phosphine chalcogenide to the solvent.

Inspection of the cadmium source,[32] while a minor contributor to the MW absorption, also shows the expected trend, where a more covalent source produces better nanocrystals (Supporting Figure 7). Reactants that are ionic are expected to show no reaction, while highly polarizable reactants will react rapidly. Analysis of a series of cadmium sources (CdSA, CdO, $CdNO_3$, $CdCl_2$) reveals the predicted trend. Only the polarizable starting precursors, CdSA, CdO, and $CdNO_3$, produce nanocrystals. The CdO is a poorer precursor we believe due to the high energy precursor activation step associated with CdO decomposition prior to nucleation of the II−VI materials. No reaction is observed for the ionic $CdCl_2$ under identical reaction conditions.

Alternate selenium precursors as also explored to accurately determine the importance of the phosphine chalcogenides precursor to this high quality synthesis. Selenourea was used as an attempt to synthesize CdSe nanocrystals in an identical methodology to the method presented in this work. Although there is evidence of growth of nanocrystals, the quality of the materials pales in comparison to our work.

The impact of the selective microwave effect is observable in the reaction rates for formation of CdSe vs CdTe nanocrystals. For the chalcogenides, the trend of reaction rate is Te reacts fastest, followed by the Se. If one considers the reactivity and bond strengths of P−Se vs P−Te, the observation is consistent with Te having a weaker covalent bond due to the increased electron density around the atom leading to a larger size. As a result, the more reactive P−Te contributes more energy into nucleating nanocrystals rather than heating the solution. This is demonstrated through the longer ramp time but much shorter reaction time.

Surprisingly a difference is observed between TBP and TOP on the surface of the nanocrystal. While on the same order of magnitude, in both cases the reactivity of TBP is slightly higher than that of TOP. This implies a difference in the nature and strength of the bonding at both the Se and the nanocrystal surface for these two ligands.[33] Considering a Tolman cone-angle argument for the tri-*n*-alkyl phosphines,[34] two plausible explanations are (1) differences in the polarizability of R_3P-X bond due to changes in the orbital hybridization in the R_3P and, more likely, (2) a decrease in packing density due to the steric interaction for the longer chained TOP. Since one would predict the cone angle, and thus electronic properties, to be essentially the same for the two systems, the steric bulk of the TOP may result in the lower rate of heating due to fewer molecular interactions. While potentially within experimental error, the reproducibility of the results suggests further investigation is needed to evaluate this empirical observation.

3.4. Stop-Flow Synthesis of II−VI Nanocrystals. The scalability of a reaction is always complicated by the presence of thermal gradients and difficulty in mixing the reactants in larger volumes.[35] This is particularly true for nanocrystal growth, where the transition of the synthetic methodology from a small reactor size (~5 mL) to a larger system (50 mL) suffers from thermal gradients in the reaction leading to larger polydispersities and poorer material performance. Microwave reactors offer an advantage over convective heat sources, due to their ability to heat without thermal gradients since selective heating is achieved by the absorption into the chalcogenide precursor triggering the nucleation event. This is accomplished in a stop-flow configuration, where the reactants are pumped into the MW cavity.

A comparison of the absorption and photoluminescence spectra for the stopped-flow dynamic and normal static reaction is shown in Figure 6. The advantage of the stopped-flow geometry is that a continuous stream of nanocrystals can therefore be generated from a stock precursor solution (>10 mg of nanocrystal/min). A disadvantage of the stop-flow system is the volume of the reactor makes heating of the solvent more difficult. The reactions require 40 min for CdSe (20 min for CdTe) due to the inability of the MW to penetrate the larger volume of solvent as well as the thickness of the reactor vessel. The slow ramp rate and lower achievable temperatures are evidence of the increased problems in reaching the desired reaction temperatures in a short period. However, the fact that the materials are the same quality supports the conclusion that the precursor absorbs the energy and transfers the heat convectively. Likewise a similar size regime can be obtained at an apparent lower reaction temperature. These observations support MW absorption by the tri-*n*-alkyl phosphine and convective losses to the solvent, particularly in light of the fact that a larger volume reactor by definition has a larger thermal sink, thus lowering the overall reaction temperature. This can be overcome by using higher microwave power or optimizing the frequency of the microwave, neither of which were explored in this manuscript.

4. Conclusion

While the microwave specific effect has been postulated, the observation of the selective nature of dielectric heating for nanocrystal growth is fascinating. If we assume the phosphine–chalcogenide is the predominant absorbing species in solution, the excess energy will activate the nucleation of cadmium–chalcogenide nanocrystals, while growth is achieved by the reaction temperature. The behaviors of time, temperature, and

(32) Qu, L; Peng, A. Z.; Peng, X. *Nano Lett.* **2001**, *1* (6), 33–337.
(33) Liu, H.; Owen, J. S.; Alivisatos, A. P. *J. Am. Chem. Soc.* **2007**, *129*, 305–312.
(34) Bunten, K. A.; Chen, L.; Fernandez, A. L.; Poe, A. *J. Coord. Chem. Rev.* **2002**, *233−234*, 41–51.
(35) (a) Yen, B. K. H.; Stott, N. E.; Jensen, K. F.; Bawendi, M. G. *Adv. Mater.* **2003**, *15* (21), 1858–1862. (b) Kawa, M.; Morii, H.; Ioku, A.; Saita, S.; Okuyama, K. J. *Nanoparticle Research* **2003**, *5* (1−2), 81–85. (c) Krishnadasan, S.; Tovilla, J.; Vilar, R.; deMello, A. J.; deMello, J. C. *J. Mater. Chem.* **2004**, *14* (17), 2655–2660. (d) Yen, B. K. H.; Gunther, A.; Schmidt, M. A.; Jensen, K. F.; Bawendi, M. G. *Angew. Chem., Int. Ed.* **2005**, *44* (34), 5447–5451.

material quality can be traced to the chemical nature of the precursors and suggest, in the reaction conditions herein, the nucleation step controls the nanocrystal formation. The observation of heating rate dependencies supports the logic of precursor activation via selective heating triggers nucleation. This is the observation of the "*specific microwave effect*" which is rarely proven. From a commercial perspective, the development of a stopped-flow synthetic methodology allows the researcher to produce high quality materials in a matter of minutes instead of hours, or continuously at a specific size and composition.

Acknowledgment. The work was supported by funding from the NIH under program EB-R01-00832, the NSF under DMR-0701462, and the Florida-Georgia Lewis Stokes Alliance for Minority Participation fellowship (A.L.W., II). We wish to thank Dr. Jeffrey A. Gerbec for helpful discussions on the use of stopped flow reactors, Dr. Steve Yun for discussions about isolation methods in nanornystal reprecipitation, and Ms. Kim Riddle for TEM analysis in the Biological Science Imaging Resource at FSU.

Supporting Information Available: Supporting Table 1 provides the heating rate data. Supporting Figure 1 illustrates low temperature synthesis in pentane. Characterization data are presented in Supporting Figures 2 (TEM) and 3 (pXRD). Supporting Figure 4 compares the microwave produced CdSe with the thermally accepted CdO grown CdSe from Peng et al. Supporting Figure 5 shows power dependent growth with both fixed and variable ramp times, and Supporting Figure 6 shows time dependent measurements of the synthetic technique. Supporting Figure 7 shows growth with alternative precursors. This information is intended to illustrate the quality of the materials produced. This material is available free of charge via the Internet at http://pubs.acs.org.

JA711115R